



## ORIGINAL ARTICLE

# Hemoglobin binding and antioxidant activity in spinal cord neurons: O-methylated isoflavone glycitein as a potential small molecule



Xiangli Luo<sup>a,b</sup>, Zhan Wang<sup>b</sup>, Jiancheng Xu<sup>c</sup>, Zhao Gao<sup>b</sup>, Zhengdong Song<sup>a</sup>,  
Wenji Wang<sup>a,\*</sup>

<sup>a</sup> The First School of Clinical Medicine of Lanzhou University, The First Hospital of Lanzhou University, Lanzhou 730000, Gansu, China

<sup>b</sup> Gansu Provincial Hospital, Lanzhou 730000, Gansu, China

<sup>c</sup> Gansu Provincial Hospital of Traditional Chinese Medicine, Lanzhou, Gansu, China

Received 22 April 2023; accepted 11 July 2023

Available online 17 July 2023

## KEYWORDS

Interaction;  
Hemoglobin;  
Glycitein;  
Spectroscopy;  
Antioxidant

**Abstract** Scientific community has been mesmerized by the application of bioactive O-methylated isoflavones with neuroprotective effects mediated by their antioxidant and antiapoptotic properties. The small size and planar-based structures allow them to interact with a wide range of biomolecules, such as DNA, lipids, and protein. Therefore, glycitein (C<sub>16</sub>H<sub>12</sub>O<sub>5</sub>), 4',7-dihydroxy-6-methoxyisoflavone, as a potential antioxidant can interact with blood proteins, especially human hemoglobin (HHb), serving as a one of the main carrier proteins. To analyze this interaction, several spectroscopic techniques as well as molecular docking analysis were used. It was revealed that glycitein can interact with HHb mediated by the formation of hydrophobic forces and main aromatic residues. Also, Y140 (A), Y35 (D), and W37 (D) were displaced to a hydrophobic microenvironment upon interaction of HHb with glycitein. Furthermore, glycitein led to a slight increase in the amount of  $\alpha$ -helix of HHb. The antioxidant assays showed that glycitein with a low concentration of 5  $\mu$ M can mitigate the neurotoxicity induced by lipopolysaccharide (LPS, 100 ng/ml) in cultured spinal cord neurons, through mitigation of lactate dehydrogenase (LDH) release, downregulation of reactive oxygen species (ROS) and malonyldialdehyde (MDA) production, recovery of superoxide dismutase (SOD) and catalase (CAT) activity, and downregulation of caspase-3 protein expression and activity. In conclusion, these data indicated that glycitein with potential pharmacological

\* Corresponding author at: No.1, Donggang West Road, Chengguan District, Lanzhou City, Gansu Province 730000, China.  
E-mail address: ldyjzwwj@163.com (W. Wang).

Peer review under responsibility of King Saud University. Production and hosting by Elsevier.



activities can potentially interact with HHb, which can be of interest for future *in vivo* studies.

© 2023 The Authors. Published by Elsevier B.V. on behalf of King Saud University. This is an open access article under the CC BY-NC-ND license (<http://creativecommons.org/licenses/by-nc-nd/4.0/>).

## 1. Introduction

Glycitein ( $C_{16}H_{12}O_5$ ), 4',7-dihydroxy-6-methoxyisoflavone with a molar mass of 284.26 g/mol, is an O-methylated isoflavone frequent presents in soy food products. Considering its potential antioxidant properties as one of the main advantages of this compound, it can be speculated that glycitein could exert favorable effects on modulation of cytotoxicity through inhibiting oxidative stress-mediated signaling pathways. For example, it has been shown that soy isoflavone, glycitein, is able to show protective effects against aggregated protein-triggered cytotoxicity and oxidative stress in transgenic *Caenorhabditis elegans* (Gutierrez-Zepeda et al. 2005). Furthermore, dietary supplementation with glycitein “during late pregnancy and lactation” could have a significant effect on the antioxidative indices (Hu et al. 2015). Recently, glycitein was reported to exert neuroprotective influences in rotenone-induced oxidative stress and apoptotic cell death *in vitro* (Dong and Yang 2022).

However, it should be emphasized that while some bioactive molecules may show potential antioxidant activity, their interaction with carrier blood proteins such as albumin, hemoglobin, and fibrinogen is not thermodynamically favorable and do not show promising pharmacokinetic activities. Therefore, it is important to evaluate the interaction of glycitein with blood proteins to obtain some preliminary information about its bioavailability, pharmacokinetic, and stability for future *in vivo* applications. Human hemoglobin (HHb) as a tetramer of globin chains with two  $\alpha$  and two  $\beta$ -chains, 572 amino acids (six Trp and ten Tyr amino acid residues), shows an  $\alpha$ -helical structure (Maurya et al. 2018). It has been reported that human HHb can serve as a drug carrier for a wide number of compounds (Ingram et al. 1962, Mandal et al. 2004). In fact, it has been shown that HHb not only acts as a carrier for oxygen but also performs the function of binding with different endogenous and exogenous molecules including drugs (Mandal et al. 2004), herbicide (Wang et al. 2007), and bioactive materials (Chowdhury et al. 2020, Sett et al. 2022). Recently, the interaction of angiotensin converting enzyme I inhibitory peptide (Sadeghzadeh et al. 2020), mancozeb as a broad-spectrum fungicide (Quds et al. 2022), phosmet as a “phthalimide derived broad spectrum organophosphate pesticide” (Kaur et al. 2023), nitrogenous disinfection byproduct haloacetonitriles (Cui et al. 2022), functionalized rhodamine (Bawa et al. 2022), noscapinoids (Panchal et al. 2023), fluorescent carbon dots (Cao et al. 2021), and flavonoid drugs (Chowdhury et al. 2020, Sett et al. 2022) with HHb has been analyzed by different spectroscopic approaches to evaluate the quenching mechanism, binding and thermodynamic parameters, as well as structural changes of protein.

Also, oxidative stress, inflammation and apoptosis are the main pathological pathways in neurological disorders (Esawy et al. 2022), especially spinal cord injury (SCI) (Guan et al. 2020). These signaling pathways play an important role in the nerve destruction processes and nerve cell death. Therefore, the inhibition of oxidative invasion can significantly reduce the occurrence of inflammation, infection, apoptosis, and as a result severe organ dysfunction (Fakhri et al. 2022, Li et al. 2023). Based on this fact, it can be deduced that treatment with strong antioxidants may improve the recovery of spinal cord patients (Fakhri et al. 2022).

Hence, in the present study, the interaction of a glycitein with HHb was evaluated by different spectroscopic techniques as well as molecular docking analysis. Also, a well-characterized SCI model *in vitro*, stimulated by lipopolysaccharide (LPS) treatment, was employed to mimic neurotoxicity in SCI. We assessed the protective effects of glycitein and the probable underlying mechanism with a focus on the oxidative stress and apoptotic pathway.

## 2. Materials and methods

### 2.1. Preparation of stock solutions

Stock solution of 100  $\mu$ M HHb (H7379, Sigma, St. Louis, MO, USA) was prepared in phosphate buffer saline (PBS, 10 mM pH = 7.4). The stock solution of 1 mM glycitein (G2785  $\geq$  97% HPLC, Sigma, St. Louis, MO, USA) was prepared in DMSO, and the volume ratios of DMSO/PBS or DMSO/cell culture medium were not exceeded 1% to not affect the structure of protein or the viability of cells.

### 2.2. Fluorescence studies

The fluorescence emission intensity of HHb (3  $\mu$ M) either alone or with different concentrations of glycitein (3–50  $\mu$ M) were read in the wavelength range of 300–440 nm. The fluorescence investigation was done at three different temperatures of 298 K, 308 K and 318 K. The HHb samples were excited at 280 nm with a fixed slit width of 5 nm. Fluorescence titration assays were done by successive titration of glycitein in a 3  $\mu$ M solution of HHb.

To correct the observed data against inner filter effects, the raw data was corrected using Eq. (1) (Ali et al. 2023):

$$F_{cor} = F_{obs} \cdot e^{(A_{ex} + A_{em})} \quad (1)$$

Where,  $F_{cor}$  and  $F_{obs}$  are the corrected and observed fluorescence intensities of HHb, respectively.  $A_{ex}$  and  $A_{em}$  are the absorbance of glycitein at excitation and emission wavelengths of HHb.

Synchronous fluorescence spectroscopy was done by fixing  $\Delta\lambda$  (wavelength interval) at 15 nm or 60 nm. The other procedures were almost similar to steady-state fluorescence study.

### 2.3. Circular dichroism (CD) study

The CD spectra of HHb in the far-UV region were read either alone or with different concentrations of glycitein (3–50  $\mu$ M) on a JASCO J-1500 spectropolarimeter at a scan rate of 100 nm  $\text{min}^{-1}$  at 298 K equipped with a cuvette path length of 1 cm. The concentration of HHb was fixed at 3  $\mu$ M while the concentration of glycitein was changed. The spectra were corrected against the ellipticity changes of blank buffer as well as glycitein solutions.

### 2.4. Molecular docking study

The molecular docking study of glycitein with HHb was carried out on a AutoDoc Vina, mainly aiming at the study of binding affinity and molecular interaction of the small molecule with the receptor. The three-dimensional (3D) crystal structure of HHb (PDB ID: 4ROL) was downloaded from the protein databank. The 3D structure of glycitein was obtained from PubChem, with a PubChem ID: 187808. The docking study was performed by setting the grid size to 76  $\times$  61  $\times$  66 Å and spacing of 1 Å to

cover the HHb residues. The conformer with the lowest docking result was chosen for docking analysis.

### 2.5. Primary cell culture

All experimental protocols were approved by the Institutional Animal Care and Use Committee and done in accordance with National Institutes of Health Guide for the Care and Use of Laboratory Animals (NIH Publications no. 80–23, revised 1996). The primary cell culture was done in accordance with previous study (Gao et al. 2016). Briefly, E18 Sprague–Dawley rats were killed, followed by dissociation and digestion of spinal cords. The cells were then centrifuged at 1000 rpm for 5 min, collected and cultivated on plates (poly-D-lysine-coated) in a mixture of minimum essential medium, 10% fetal bovine serum, 0.6% glucose, and 1% antibiotics. After 24 h, the medium was replaced with neurobasal media including B27, GlutaMAX, and antibiotics (Gibco Lab, Grand Island, NY) in a humidified 5% CO<sub>2</sub> incubator at 37 °C. The neurons were cultured for 8 days and then used for further experiments.

### 2.6. MTT and lactate dehydrogenase (LDH) assays

The cultured spinal cord neurons were incubated with different concentrations of (0, 1, 5, 10, 20, 50 μM) glycitein for 24 h. After determining the optimal safe concentration, by MTT assays as explained below, the neurons were co-treated with a fixed concentration of glycitein and 100 ng/ml LPS (Sigma, St. Louis, MO, USA) for 24 h. MTT assay was done to assess the cell viability. After culturing and treating the cells into a 96-well plate for 24 h, the old medium was replaced with 100 μL of 0.5 mg/mL MTT reagent and the cells were incubated in the CO<sub>2</sub> incubator at 37 °C for 4 h. Then 100 μL DMSO was added to the cells and the optical density of samples was measured using a plate reader (Bio-Tek Instruments Inc.) at 570 nm and the absorbance were normalized to controls. Lactate dehydrogenase (LDH) release was assessed with LDH Detection Kit (cat. no. ab65393; Abcam) according to the manufacturer's procedure described in a previous study (Qian and Yang 2022).

### 2.7. Measurement of ROS generation

The spinal cord neurons were incubated with 2,7-dichlorofluorescein diacetate (DCF-DA) (Sigma, St. Louis, MO, USA) with a concentration of 10 μM for 50 min at 37 °C in the dark. Intracellular ROS generation after resuspension of cells in PBS was detected using a Flx 8000 Bio-Tek fluorometer (Bio-tek Instruments Inc., Winooski, VT) with an excitation wavelength of 480 nm and an emission wavelength of 530 nm.

### 2.8. Measurement of lipid peroxidation

Malonyldialdehyde (MDA) as an important index of lipid peroxidation was measured by using MDA Assay Kit (Colorimetric, ab118970) based on the manufacturer's instructions. The absorbance of the samples was read on a microplate reader (Bio-Tek Instruments Inc.). The data were presented as multiples of the control value.

### 2.9. Measurement of antioxidant enzyme activity

The superoxide dismutase (SOD) and catalase (CAT) activity were assessed by application of commercially available assay kits, SOD Activity Assay Kit (Colorimetric, ab65354) and CAT Activity Assay Kit (Colorimetric, ab83464), following the manufacturer's instructions. Protein concentration was calculated by using a BCA protein kit (Jiancheng Bioengineering Institute, Nanjing, China). The enzyme activities were then presented as multiples of the control value.

### 2.10. Western blot assay

Western blot analysis was done as previously explained with some modifications. (Nie et al. 2006). Briefly, spinal cord neurons were washed, lysed, incubated on ice for 30 min, centrifuged at 16,000 × g for 10 min at 4 °C, and the supernatant was used for Western blot. Total protein concentration was assessed on a BCA assay kit (Jiancheng Bioengineering Institute, Nanjing, China). For detection of activated caspase-3, 30 μg of extracted protein samples were loaded and separated by sodium dodecyl sulfate–polyacrylamide gel electrophoresis (SDS–PAGE), followed by transferring to polyvinylidene difluoride membranes, blocking with 5% non-fat dry milk in Tris–buffered saline (TBS) for 1 h at ambient temperature, probing with rabbit anti-active caspase-3 (1:1000; Abcam) antibody and anti-β-actin (1:1000; Abcam) overnight at 4 °C, and incubating with an anti-rabbit IgG–HRP secondary antibody (1:1000) for 1 h at ambient temperature. Bands were finally detected using ECL kit upon exposure to X-ray film.

### 2.11. Caspase-3 activity detection

After cultivation and treating with glycitein or 100 ng/ml LPS, as mentioned before, the activity of caspase-3 was assessed by the Caspase-3 detection kit (#ab39401, Abcam, Cambridge, UK) according to the supplier's instructions as described previously (Rao et al. 2023).

### 2.12. Statistical analysis

One-way ANOVA was used to compare the data, reported as mean ± SD of three experiments, between untreated and treated groups.  $P < 0.05$  was considered statistically significant.

## 3. Result and discussion

### 3.1. Determining the quenching, binding and thermodynamic parameters

HHb contains an intrinsic fluorescence characteristic owing to the presence of aromatic residues, including tryptophan (Trp) and tyrosine (Tyr), which emit fluorescence signals at around 340 nm and 307 nm, respectively, when the excitation wavelength was fixed at 280 nm (Shen et al. 2007). However, Tyr residues due to low quantum yield exhibit minimal fluorescence in comparison with the Trp residues (Chen and Cohen 1966, Koifman et al. 2022). Therefore, upon excitation of proteins at 340 nm, Trp residues mostly yield the maximum emis-

sion (Singh et al. 2023). Upon addition of a ligand into the protein solution, the fluorescence characteristic of the fluorophore, mainly Trp, may alter in accordance with the alterations in its microenvironment, which depends on the binding affinity of the ligand (Cazacu et al. 2022). In other words, the quenching rate of the proteins by ligands depends on the type of interaction between these two molecules dictated by a number of intrinsic and extrinsic factors such as stability of protein as well as of the pH of medium (Zhang et al. 2022). Fig. 1 displays the corrected fluorescence intensities of HHb at 298 K with different concentrations of glycitein at an excitation wavelength of 280 nm. It was found that there was a continuous quenching in the fluorescence intensity of HHb after addition of increasing concentrations of glycitein, revealing the microenvironmental changes around aromatic residues, especially Trp and Try. Furthermore, it was seen that there was around 5 nm blue shift in the maximum emission wavelength after addition of highest concentrations of glycitein (50  $\mu\text{M}$ ) to HHb solution (3  $\mu\text{M}$ ), indicating a more nonpolar environment for aromatic residues for HHb after complexation with glycitein in comparison with that of free protein (Nishinami et al. 2022).

The analysis of the fluorescence quenching data was performed to evaluate the type of fluorescence quenching along with the binding and thermodynamic constants.

Fluorescence emission quenching can be determined by using the well-known Stern–Volmer Eq. (2) as follows (Zhang et al. 2023):

$$F_0/F = 1 + K_{SV}[Q] = 1 + k_q\tau_0[Q] \quad (2)$$

where  $F_0$ , and  $F$  define the fluorescence intensities of protein in the absence and presence of ligand (glycitein),  $[Q]$  is the concentration of ligand, and  $K_{SV}$ ,  $k_q$ , and  $\tau_0$  are known as the Stern–Volmer quenching constant, the biomolecular

quenching constant, and the lifetime of the aromatic residues (around  $6 \times 10^{-9} \text{ s}^{-1}$ ), respectively. The linear regression of Eq. (2) derived from plotting of  $F_0/F$  vs. [glycitein] can be used to calculate the values of  $K_{SV}$  and  $k_q$ .

The Stern–Volmer plots of HHb quenching by glycitein at an excitation wavelength of 280 nm were shown in Fig. 2. The obtained curves showed a good linearity in the studied concentration range of glycitein. Therefore, the calculated values of  $K_{SV}$  and  $k_q$  were summarized in Table 1. There was a remarkable difference between the values of  $K_{SV}$  and  $k_q$  at three different temperatures (Table 1).

In fact, it was exhibited that values of  $K_{SV}$  for interaction of HHb and glycitein were  $1.01 \times 10^5 \text{ M}^{-1}$ ,  $0.80 \times 10^5 \text{ M}^{-1}$ , and  $0.41 \times 10^5 \text{ M}^{-1}$  at 298 K, 308 K, and 318 K, respectively. The value of the  $K_{SV}$  at 298 K was around 2.46-fold higher than that of the 318 K. Also, the values of  $k_q$  were determined to be  $1.68 \times 10^{13} \text{ M}^{-1} \text{ s}^{-1}$ ,  $1.33 \times 10^{13} \text{ M}^{-1} \text{ s}^{-1}$ , and  $0.68 \times 10^{13} \text{ M}^{-1} \text{ s}^{-1}$  at 298 K, 308 K, and 318 K, respectively. To explore the type of quenching mechanism, it is clearly evident from the values of  $k_q$  (Table 1) that these values are  $10^2$ – $10^3$  magnitude higher than the maximum diffusion-controlled limit,  $1 \times 10^{10} \text{ M}^{-1} \text{ s}^{-1}$ . Also, there is a reverse dependency between values of  $K_{SV}$  and temperature elevation, which all these data reveal that the mechanism contributing to the HHb- glycitein interaction is the static type (Khan et al. 2023).

The binding constant ( $k_b$ ) and the number of binding sites ( $n$ ) could be estimated using the double logarithmic modified Stern–Volmer Eq. (3) as follows (Zeinabad et al. 2016):

$$\lg F_0 - F/F = \lg kb + n \log[Q] \quad (3)$$

The plots of  $\log(F_0 - F)/F$  vs.  $\log[\text{glycitein}]$  are shown in Fig. 3 and the respective values of binding constants are summarized in Table 2. In this analysis we have also observed the good linearity, corresponding to the one bonding site on the

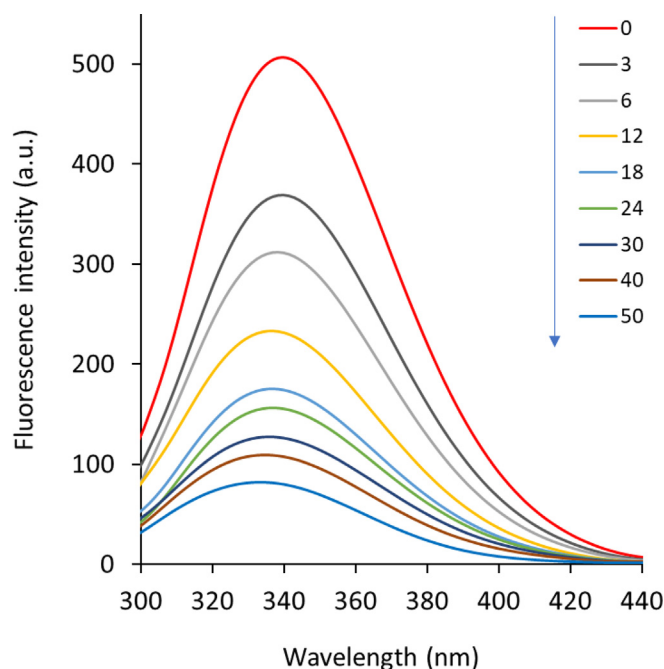


**Fig. 1** Fluorescence quenching study of HHb upon interaction with different concentrations of glycitein at room temperature.  $C_{HHb}$ : 3  $\mu\text{M}$ ,  $C_{glycitein}$ : 3–50  $\mu\text{M}$ .

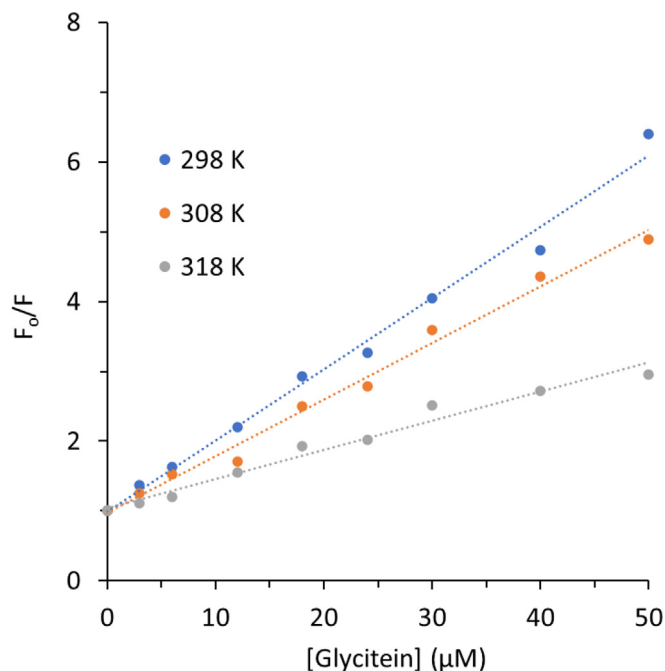


**Fig. 2** Stern-Volmer plots of HHb upon interaction with different concentrations of glycitein at three temperatures.  $C_{HHb}$ : 3  $\mu\text{M}$ ,  $C_{glycitein}$ : 3–50  $\mu\text{M}$ .

**Table 1** Values of  $K_{SV}$  and  $k_q$  for interaction of HHb and glycitein at different temperatures.

T (K)	$K_{SV} (\text{M}^{-1}) \times 10^5$	$k_q (\text{M}^{-1} \text{s}^{-1}) \times 10^{13}$
298	1.01	1.68
308	0.80	1.33
318	0.41	0.68

HHb structure for glycitein (Li et al. 2022). The values of  $k_b$  and  $n$  were changed after increasing of temperature, indicating the less stability of HHb-glycitein complex at 298 K relative to that of 318 K.

This can be described based on the basis that conformational changes could heavily influence the binding affinity of HHb to ligand and the elevation of temperature may play a key role in the binding of the glycitein as a result of conforma-

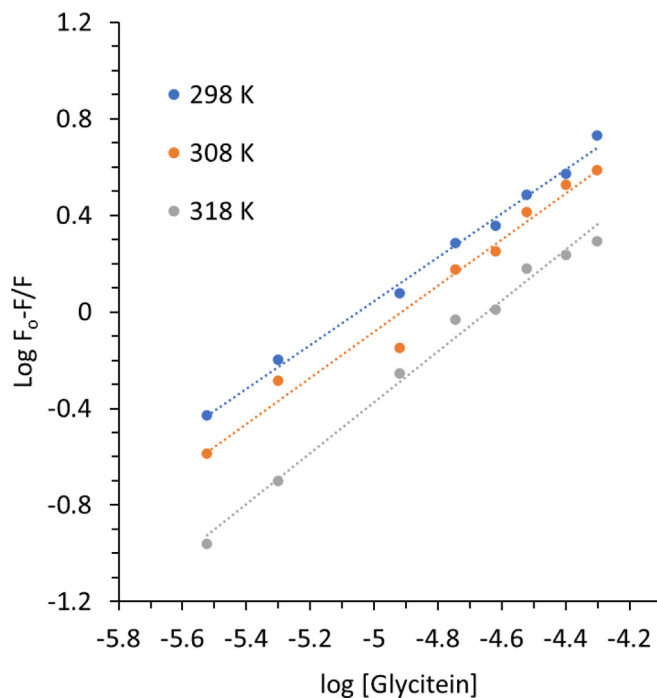


**Fig. 3** Modified Stern-Volmer plots of HHb upon interaction with different concentrations of glycitein at three temperatures.  $C_{HHb}$ : 3  $\mu\text{M}$ ,  $C_{glycitein}$ : 3–50  $\mu\text{M}$ .

**Table 2** Values of  $K_b$  and  $n$  for interaction of HHb and glycitein at different temperatures.

T (K)	$\lg K_b$	$n$
298	4.59	0.91
308	4.69	0.95
318	4.88	1.05

tional alterations in higher temperatures in comparison to lower temperatures. Therefore, it can be supposed that the elevation of temperature may increase the affinity of glycitein at the ligand binding site of HHb. The quenching and binding parameters were shown to have the lowest value in the case of the interaction of glycitein with the HHb at 298 K, mainly due to the less exposure of binding site at lower temperature in comparison with higher temperature; because of that, glycitein experienced more steric hindrance for its binding inside protein (Wang and Cheng 2022, Zhang et al. 2023).

Furthermore, it was seen that there was almost one binding site in HHb for binding to glycitein. Also, the magnitude of the value of  $K_b$  for the interaction of HHb and glycitein was around  $10^4$ , disclosing a moderate binding affinity (Cazacu et al. 2022) between this protein and studied ligand, glycitein.

Thermodynamic parameters [standard enthalpy change ( $\Delta H^\circ$ ), standard entropy change ( $\Delta S^\circ$ ) and standard free energy change ( $\Delta G^\circ$ )] were also calculated using the well-known Van't Hoff Eq. (4) and Gibbs-Helmholtz Eq. (5) as follows (Kaur et al. 2023):

$$\ln Kb = -\Delta H^\circ / RT + \Delta S^\circ / R \quad (4)$$

$$\Delta G^\circ = \Delta H^\circ - T\Delta S^\circ \quad (5)$$

The Van't Hoff plots were used to calculate the values of  $\Delta H^\circ$  and  $\Delta S^\circ$  (Fig. 4). It was disclosed that the interaction of glycitein at the binding site was done with positive values

**Table 3** Values of  $\Delta H^\circ$ ,  $\Delta S^\circ$ , and  $\Delta G^\circ$  for the interaction of HHb and glycitein at different temperatures.

T (K)	$\Delta H^\circ$ (kJ/mol)	$\Delta S^\circ$ (J/mol. K)	$\Delta G^\circ$ (kJ/mol)
298	26.13	174.96	-26.00
308	26.13	174.96	-27.75
318	26.13	174.96	-28.97

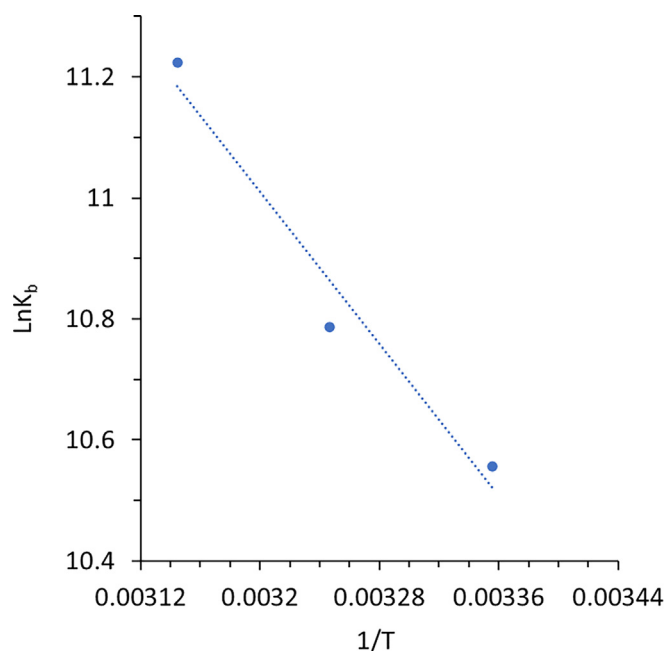
of  $\Delta H^\circ$  (26.13 kJ/mol) and  $\Delta S^\circ$  (174.96 J/mol K). However, the value of  $\Delta G^\circ$  was negative with a value of -26.00 kJ/mol (Table 3).

From the values of  $\Delta H^\circ$ ,  $\Delta S^\circ$ , and  $\Delta G^\circ$ , it can be inferred that the positive values of  $\Delta H^\circ$  (26.13 kJ/mol) and  $\Delta S^\circ$  (174.96 J/mol K) are characteristics of the contribution of hydrophobic forces (Kaur et al. 2023, Khan et al. 2023) in the formation of HHb- glycitein complex. It should be also noted that, there might be some other physical forces contributing such as electrostatic interaction and hydrogen bonding, however less interacting.

### 3.2. Evaluation of the structural changes of Hb

#### 3.2.1. Synchronous fluorescence study for conformational changes of HHb

Synchronous fluorescence spectroscopy has been widely used as a valuable approach to study ligand-mediated changes in the microenvironment surrounding Tyr and Trp amino acid residues present in proteins (Mavani et al. 2022). The blue or red shift in the position of maximum emission wavelength derived from synchronous fluorescence study exhibits the changes in polarity around these aromatic residues (Salam et al. 2023). When the values of  $\Delta\lambda$  are fixed at 15 or 60 nm, synchronous fluorescence spectra give some information regarding polarity alterations in the microenvironment around

**Fig. 4** Van't Hoff plot of HHb upon interaction with different concentrations of glycitein at three temperatures.

Tyr and Trp amino acid residues, respectively (Salam et al. 2023). The synchronous fluorescence spectra of HHb either alone or with different concentrations of glycitein with  $\Delta\lambda$  of 15 nm and 60 nm are exhibited in Fig. 5. The addition of  $\Delta\lambda$  triggered a reduction in emission intensities of HHb, which reveals that the small molecule interacted with HHb and considerably quenched the intrinsic fluorescence of Tyr and Trp aromatic acid residues. The positions associated with maximum emission peaks of Tyr (Fig. 5a) and Trp (Fig. 5b) residues were apparently changed after interaction with increasing concentrations of glycitein, specifying the microenvironmental changes around both Tyr and Trp residues of HHb. In fact, a blue shift in the position of maximum emission peak of synchronous fluorescence spectra demonstrates a decrease in the polarity around aromatic residues (Banu et al. 2022).

Thus, the data suggested that the interaction of glycitein with HHb resulted in a rearrangement of both Tyr and Trp residues placed in a hydrophilic environment to a more hydrophobic cavity. In fact, the hydrophobic portions play a key role in modulating the binding of oxygen molecules to HHb, intensifying the hydrophobic environment surrounding aromatic amino acid residues presented in the vicinity of oxygen binding cavity may apparently influence the oxygen-carrying ability of HHb (Cui et al. 2022, Lyndem et al. 2023).

### 3.2.2. Circular dichroism (CD) study for secondary structural changes of HHb

Interaction of proteins with ligands might result in some secondary structural changes in proteins (Kaur et al. 2023). Therefore, to further analyze the effect of glycitein on the secondary structure of HHb, CD analysis was carried out in the range of 260–190 nm at different concentrations of glycitein. Far-UV CD analysis was done for HHb either alone or HHb-glycitein samples. The spectra (Fig. 6) show two characteristic minima at 208 nm and 222 nm, corresponding to  $\pi$ - $\pi^*$  and  $n$ - $\pi^*$  transitions of the  $\alpha$ -helical conformer, respectively (Kong et al. 2023, Shahabadi et al. 2023).

As shown in Fig. 6, the CD spectra of HHb in the presence and absence of glycitein displayed that the shapes and positions of minima altered negligibly, indicating that the secondary structure of the protein remained predominantly intact (Mariam et al. 2017). The  $\alpha$ -helical content of HHb revealed a slight increase from 56.33% for free HHb to 59.99% for HHb-glycitein (50  $\mu$ M) sample, suggesting a slight changes in the secondary structure of the HHb molecule or the

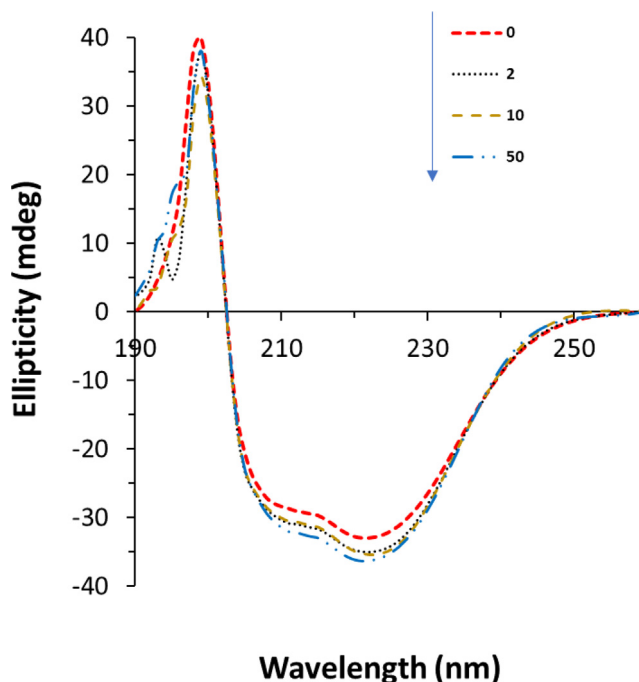


**Fig. 6** Circular dichroism study of HHb upon interaction with different concentrations of glycitein at room temperature.  $C_{HHb}$ : 3  $\mu$ M,  $C_{glycitein}$ : 3–50  $\mu$ M.

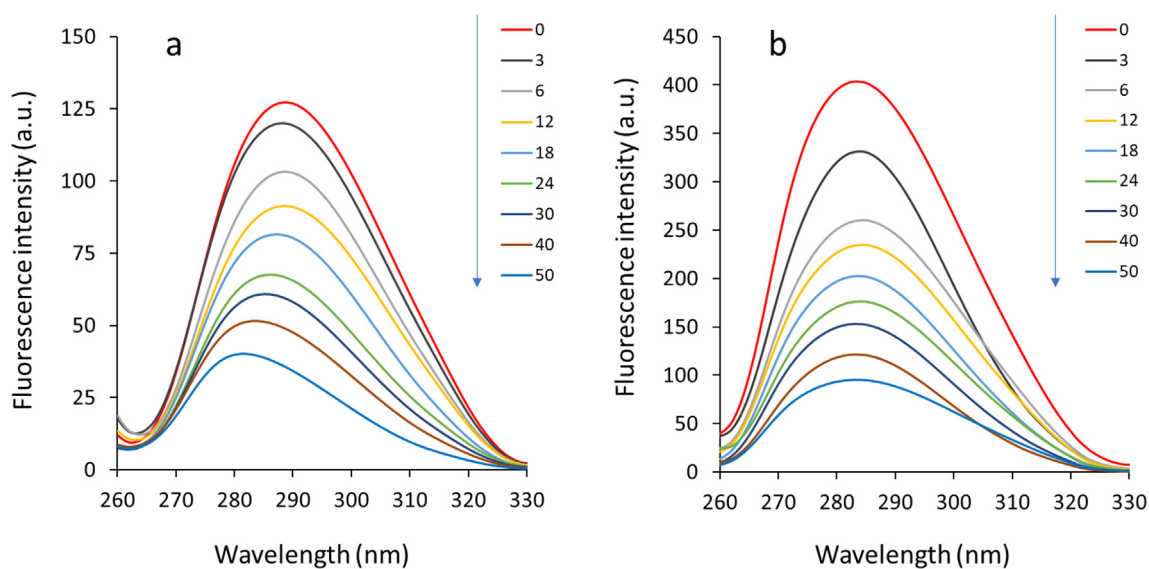


**Fig. 5** Synchronous fluorescence study of HHb upon interaction with different concentrations of glycitein at room temperature. (a)  $\Delta\lambda = 15$  nm. (b)  $\Delta\lambda = 60$  nm.  $C_{HHb}$ : 3  $\mu$ M,  $C_{glycitein}$ : 3–50  $\mu$ M.

probability of a higher stability of HHb-glycitein complex than free HHb.

### 3.3. Amino acid residues in the binding pocket

Molecular docking study can provide useful information about the theoretical representation of the binding properties of small molecules to proteins (Chaudhuri et al. 2011, Precupas et al. 2022). Indeed, molecular docking could be used as a complementary study to support the experimental data (Salam et al. 2023). Therefore, the binding mode of glycitein with HHb was investigated theoretically using molecular docking study.

The best dock score of  $-8.0$  kcal/mol ( $= -33.46$  kJ mol $^{-1}$ ) was determined theoretically for the interaction of glycitein with HHb (Fig. 7). This docking result was higher than the  $\Delta G^\circ$  value ( $-26.00$  kJ mol $^{-1}$  at 298 K) calculated based on fluorescence spectroscopy as summarized in Table 3, which may derive from the more complexity of experimental procedure

than theoretical approaches. Among the 10 different conformations of the HHb-glycitein complexes, the one with the best (highest) docking score is exhibited in Fig. 7.

The best docked structure was further analyzed for determining the bimolecular interactions of the glycitein with the amino acid residues located on the binding site of HHb and the outcomes of these interactions is depicted in Fig. 7 (HHb-glycitein complex). It was observed from Fig. 7, that the glycitein molecule showed both hydrophobic and hydrogen bonding interactions with the relevant amino acid residues located in the binding site of HHb. The results of the docking study showed the hydrophobic interactions of the C11, C7, C7, C14, and C12 atoms of glycitein with P95 (A), Y140 (A), R141 (A), Y35 (D), and W37 (D) amino acid residues of HHb, respectively. Also, it was shown that O4, O4, O3, O5, O2, O4, and O4 atoms of glycitein contribute in the formation of hydrogen bonding with S138 (A), R141 (A), R141 (A), K99 (C), V1 (C), R141 (A), and V1(C), respectively. As, synchronous fluorescence spectroscopy study showed that aro-

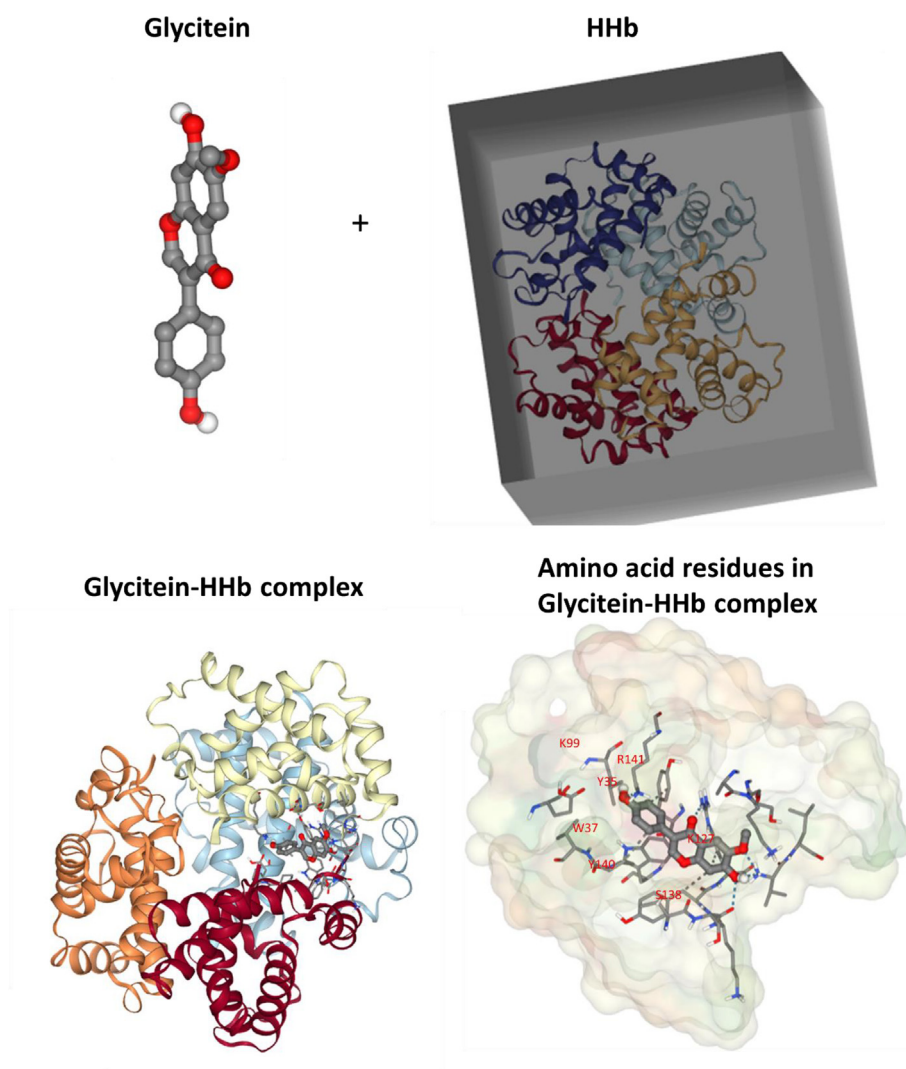
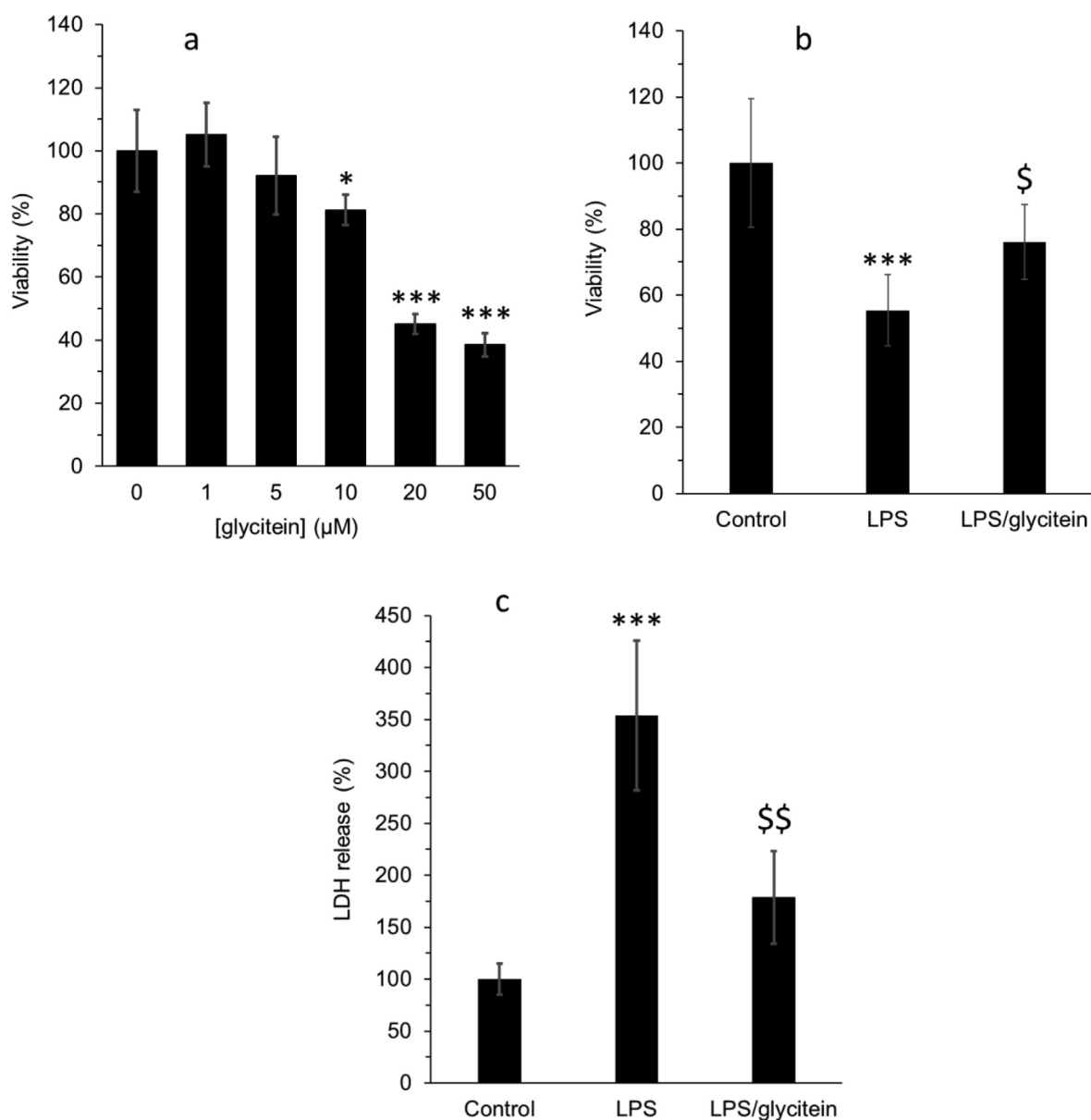


Fig. 7 Molecular docking study of HHb upon interaction with glycitein.



**Fig. 8** (a) Effect of different concentrations of (1–50 μM) glycitein on the viability of cultured spinal cord neurons after 24 h, determined by MTT assay. (b) Cell viability analysis using MTT assay in cultured spinal cord neurons after 24 h treatment with LPS (100 ng/mL) without or with co-treatment with glycitein (5 μM). (c) Membrane damage evaluation using LDH assay in cultured spinal cord neurons after 24 h treatment with LPS (100 ng/mL) without or with co-treatment with glycitein (5 μM). Each data expresses the mean ± SEM (n = 3). \*  $p < 0.05$ , and \*\*\*  $p < 0.001$ , significant difference versus negative control cells; \$  $p < 0.05$  and \$\$  $p < 0.01$ , significant difference versus LPS-treated group.

matic residues of HHb experienced microenvironmental changes after interaction with glycitein, it can be deduced from molecular docking analysis that these residues were Y140 (A), Y35 (D), and W37 (D), which have been displaced to a more hydrophobic environment after interaction with glycitein.

#### 3.4. The protective effects of glycitein against LPS-stimulated neurotoxicity

To determine the maximum nontoxic concentration of glycitein against primary cultured spinal cord neurons, the cells were incubated with different concentrations of primary cul-

tured spinal cord neurons for 24 h. Fig. 8a showed that glycitein with concentrations of 1 μM and 5 μM induced no significant cytotoxic effects against neuron culture relative to control cells, whereas at higher concentrations of 10 μM, 20 μM, and 50 μM, glycitein triggered a significant neurotoxic effect after 24 h. Therefore, glycitein with a concentration of 5 μM was used for further experiments. To explore the promising protective effects of glycitein against LPS-stimulated neurotoxicity, primary cultured spinal cord neurons were co-treated with 5 μM glycitein as well as 100 ng/ml LPS. The results of MTT showed that glycitein treatment significantly mitigated the neuronal loss stimulated by LPS (Fig. 8b). Also,

it was shown that glycitein significantly reduced the level of LDH release induced by LPS (Fig. 8c). Therefore, it may be suggested that glycitein can recover the values of cell viability through modulation of cell membrane damage induced by LPS.

### 3.5. Antioxidative activity of glycitein

To determine the protective effects induced by glycitein was assisted by antioxidative properties, we first assessed the intracellular level of ROS production after LPS treatment (Fig. 9a). The increased DCF intensity as a criterion for ROS overproduction after LPS incubation was decreased by glycitein co-treatment. A significant reduction in the level of MDA formation was also detected in glycitein treated neurons overexpressed by LPS (Fig. 9b), demonstrating that glycitein seems to inhibit lipid peroxidation stimulated by oxidative stress. Furthermore, we assessed the effects of glycitein on the activity of endogenous antioxidant system, SOD and CAT, and the

outcomes exhibited that the reduced enzymatic activities of SOD (Fig. 9c) and CAT (Fig. 9d) were recovered by glycitein co-treatment.

### 3.6. Antiapoptotic activity of glycitein

To examine the possible antiapoptotic activity of glycitein in cultured spinal cord neurons, the expression of caspase-3 protein was analyzed by western blot after LPS and glycitein treatment (Fig. 10a). As shown in Fig. 10a, the increased expression of activated caspase-3 induced by LPS was decreased by glycitein. In addition, by assessing the activity of caspase-3, we found that the activity of this enzyme was reduced after co-treatment of LPS-treated cells with glycitein (Fig. 10b). Our data showed that LPS-stimulated neuronal death in spinal cord neurons was significantly modulated through downexpression of caspase-3 protein and associated activity, as evidenced by western blot analysis and enzyme activity assay, respectively.

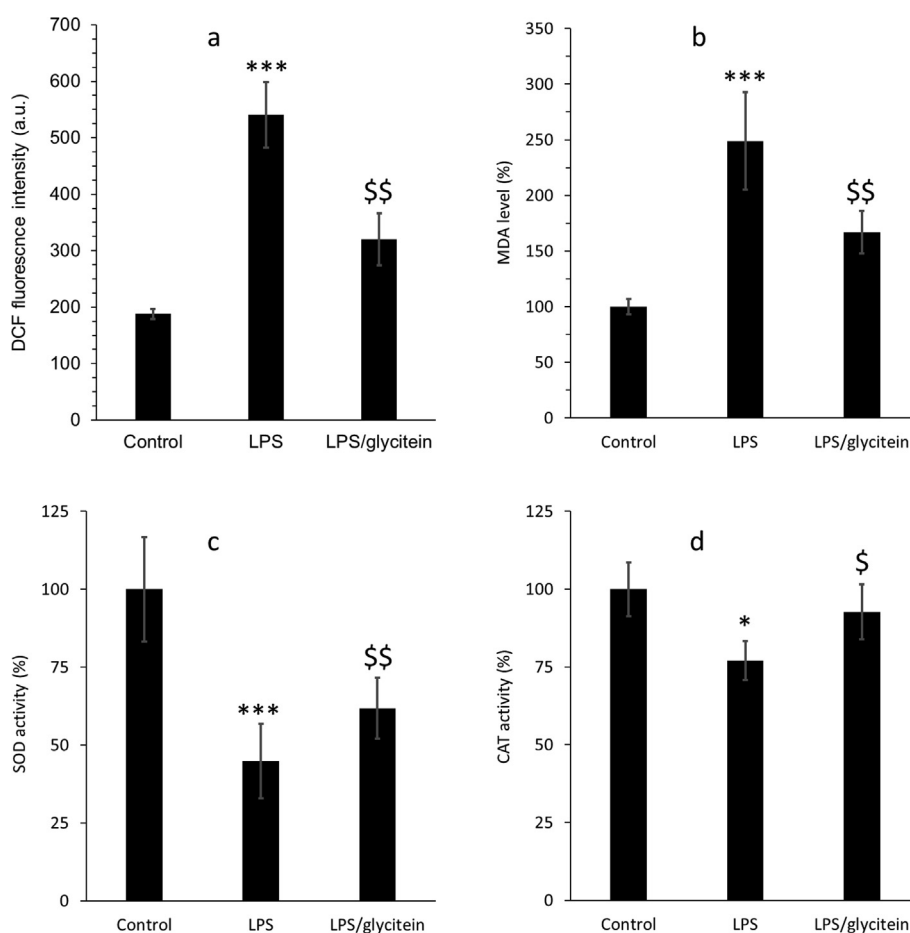


**Fig. 9** (a) The evaluation of intracellular ROS level using DCF fluorescence test in cultured spinal cord neurons after 24 h treatment with LPS (100 ng/mL) without or with co-treatment with glycitein (5  $\mu$ M). (b) The investigation of lipid peroxidation using MDA assay in cultured spinal cord neurons after 24 h treatment with LPS (100 ng/mL) without or with co-treatment with glycitein (5  $\mu$ M). (c) The investigation of SOD activity in cultured spinal cord neurons after 24 h treatment with LPS (100 ng/mL) without or with co-treatment with glycitein (5  $\mu$ M). (d) The investigation of CAT activity in cultured spinal cord neurons after 24 h treatment with LPS (100 ng/mL) without or with co-treatment with glycitein (5  $\mu$ M). Each data expresses the mean  $\pm$  SEM (n = 3). \*  $p$  < 0.05, and \*\*\*  $p$  < 0.001, significant difference versus negative control cells; \$  $p$  < 0.05 and \$\$  $p$  < 0.01, significant difference versus LPS-treated group.

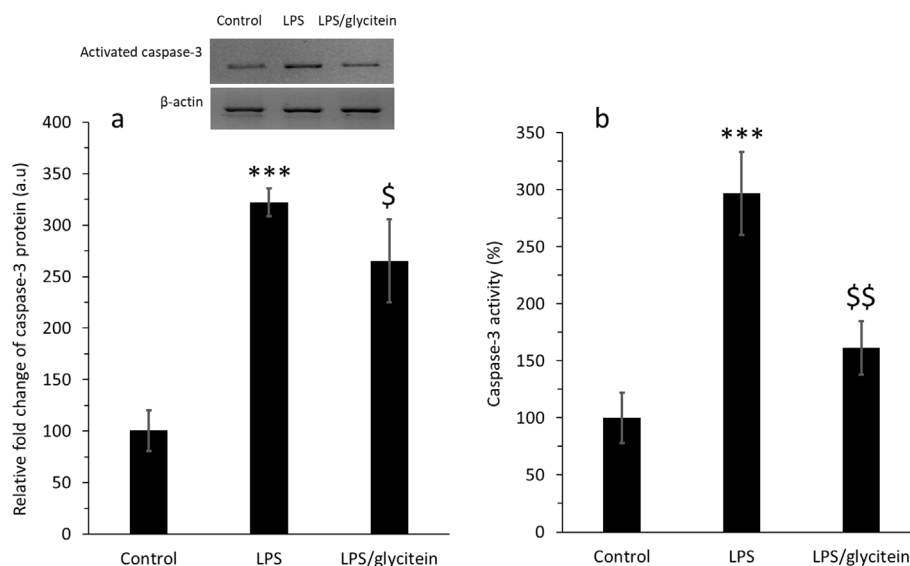


**Fig. 10** (a) The evaluation of activated caspase-3 in the protein level using western blot analysis in cultured spinal cord neurons after 24 h treatment with LPS (100 ng/mL) without or with co-treatment with glycitein (5  $\mu$ M). (b) The investigation of caspase-3 activity in cultured spinal cord neurons after 24 h treatment with LPS (100 ng/mL) without or with co-treatment with glycitein (5  $\mu$ M). Each data expresses the mean  $\pm$  SEM (n = 3). \*\*\*  $p$  < 0.001, significant difference versus negative control cells; \$  $p$  < 0.05 and \$\$  $p$  < 0.01, significant difference versus LPS-treated group.

Indeed, treatments for neurological disorders and injuries, particularly SCI, remain unsolved so far and are regarded as major clinical challenges (Blight et al. 2019). Part of these challenges stem from the complex pathophysiological mechanisms involved in SCI treatment. As a result, developing new treatments that target the primary mechanisms involved in SCI is of particular clinical importance. For this reason, the discovery of strong antioxidant compounds is an attractive and promising strategy for the treatment of SCI (Yousefpour et al. 2023). Natural antioxidants have been tested as potential alternatives or complementary treatments for some neurological injuries, including SCI, in preclinical studies (Coyoy-Salgado et al. 2019). But about their effectiveness as natural antioxidants and their neuroprotective effects, not enough is known yet, and more importantly, although these compounds have been tested in animal models with promising results, not many clinical studies has been done on humans (Coyoy-Salgado et al. 2019). Because most of these plants are available around the world at a much lower cost than some synthetic drugs used to treat SCI, it is critical to develop some strategies to study the effects of these natural compounds in SCI.

Relied on *in vitro* experimental model of SCI, the present report aimed to explore the function of glycitein in spinal cord neurons exposed to LPS, a potential agent induces oxidative stress response. Our data furnish potential outcomes that application with glycitein protects cultured spinal cord neurons against oxidative stress and apoptosis stimulated by LPS treatment. We also demonstrated that mechanistically, glycitein decreases the generation of ROS and MDA through recovering of SOD and CAT activity, and thereby inhibits the activation end expression of caspase-3 following LPS treatment. As glycitein has a hydrophobic nature, it can easily cross the cell membrane and regulate several signaling pathways (Ziberna et al. 2014). Therefore, glycitein can be applied *in vitro* studies to directly interact with cultured cells to evaluate its protective role against oxidative stress. The concentra-

tion of glycitein used in the cellular part was 5  $\mu$ M, which is readily obtainable from a daily diet, making our results more clinically relevant. Glycitein has shown potential antioxidant and neuroprotective effects in the cellular model of Parkinson's disease (Dong and Yang 2022). Additionally, glycitein possesses anti-apoptotic activities against isoproterenol-treated cardiomyoblast cells mediated by p38 and NF $\kappa$ B signaling pathway (Lin et al. 2013). Therefore, all these studies in line with our results suggest that glycitein can be used as a potential bioactive compound against oxidative stress-induced neurotoxicity. Finally, it should be emphasized that while we exhibited the protective impacts of glycitein against spinal cord neuronal toxicity, these outcomes encounter a one serious limitation as the experiments modeled in this report are based on *in vitro* assays, in which the cell microenvironment is completely different from *in vivo* condition and the neurotoxicity following SCI cannot be mimicked properly.

#### 4. Conclusion

In this study, the interaction of glycitein with HHb was studied by different spectroscopic as well as molecular docking studies. Also, the antioxidant activity of glycitein against LPS-induced oxidative stress in cultured spinal cord neurons was evaluated by several cellular assays. The data showed that glycitein can potentially bind with HHb and induced no significant changes in the protein structure and only resulted in slight conformational changes around Y140 (A), Y35 (D), and W37 (D) amino acid residues. Also, cellular assays showed that the neurotoxicity induced by LPS in cultured spinal cord neurons can be mitigated by glycitein through regulation of membrane leakage, oxidative stress, and apoptosis. This study may hold great promise for the development of glycitein-based products in therapeutic applications. However, the penetration of glycitein through blood-spinal cord barrier (BSCB), the main equivalent of the blood-brain barrier (BBB), should be explored in the future studies to may provide further relevant information for clinical applications.

## Funding

This study was supported by Gansu Province Youth Science and Technology Plan (21JR7RA635).

## Declaration of Competing Interest

The authors declare that they have no known competing financial interests or personal relationships that could have appeared to influence the work reported in this paper.

## References

- Ali, M.S., Rehman, M.T., Al-Lohedan, H.A., Alajmi, M.F., 2023. Study of the Binding of Cuminaldehyde with Bovine Serum Albumin by Spectroscopic and Molecular Modeling Methods. *J. Spectrosc.* 2023.
- Banu, A., Khan, R.H., Qashqoosh, M.T.A., Manea, Y.K., Furkan, M., Naqvi, S., 2022. Multispectroscopic and computational studies of interaction of bovine serum albumin, human serum albumin and bovine hemoglobin with bisacodyl. *J. Mol. Struct.* 1249, 131550.
- Bawa, R., Deswal, N., Kumar, A., Kumar, R., 2022. Scrutinizing the interaction of bovine serum albumin and human hemoglobin with isatin-triazole functionalized rhodamine through spectroscopic and In-silico approaches. *J. Mol. Liq.* 360, 119558.
- Blight, A.R., Hsieh, J., Curt, A., Fawcett, J.W., Guest, J.D., Kleitman, N., Kurpad, S.N., Kwon, B.K., Lammertse, D.P., Weidner, N., 2019. The challenge of recruitment for neurotherapeutic clinical trials in spinal cord injury. *Spinal Cord* 57 (5), 348–359.
- Cao, L., Li, J., Song, Y., Cong, S., Wang, H., Tan, M., 2021. Molecular interaction of fluorescent carbon dots from mature vinegar with human hemoglobin: Insights from spectroscopy, thermodynamics and AFM. *Int. J. Biol. Macromol.* 167, 415–422.
- Cazacu, N., Chilom, C.G., David, M., Florescu, M., 2022a. Conformational changes in the BSA-LT4 complex induced by the presence of vitamins: Spectroscopic approach and molecular docking. *Int. J. Mol. Sci.* 23 (8), 4215.
- Cazacu, N., Stan, D.L., Tărcă, R., Chilom, C.G., 2022b. Binding of flavonoids to yeast aldehyde dehydrogenase: a molecular mechanism and computational approach. *J. Biomol. Struct. Dyn.*, 1–8.
- Chaudhuri, S., Chakraborty, S., Sengupta, P.K., 2011. Probing the interactions of hemoglobin with antioxidant flavonoids via fluorescence spectroscopy and molecular modeling studies. *Biophys. Chem.* 154 (1), 26–34.
- Chen, R.F., Cohen, P.F., 1966. Quenching of tyrosine fluorescence in proteins by phosphate. *Arch. Biochem. Biophys.* 114 (3), 514–522.
- Chowdhury, S., Bhuiya, S., Haque, L., Das, S., 2020. In-depth investigation of the binding of flavonoid taxifolin with bovine hemoglobin at physiological pH: Spectroscopic and molecular docking studies. *Spectrochim. Acta A Mol. Biomol. Spectrosc.* 225, 117513.
- Coyoy-Salgado, A., Segura-Urbe, J.J., Guerra-Araiza, C., Orozco-Suárez, S., Salgado-Ceballos, H., Feria-Romero, I.A., Gallardo, J. M., Orozco-Barrios, C.E., 2019. The importance of natural antioxidants in the treatment of spinal cord injury in animal models: an overview. *Oxid. Med. Cell. Longev.* 2019.
- Cui, J., Xu, Y., Yu, H., Lv, Z., Wang, J., Zong, W., 2022. A pipeline to evaluate the discrepant interactions between typical nitrogenous disinfection byproduct haloacetonitriles and human hemoglobin. *Biophys. Chem.* 289, 106876.
- Dong, N., Yang, Z., 2022. Glycitein exerts neuroprotective effects in Rotenone-triggered oxidative stress and apoptotic cell death in the cellular model of Parkinson's disease. *Acta Biochim. Pol.* 69 (2), 447–452.
- Esawy, A., Eltablawy, N.A.A., El-Fattah, A., Abdalwahab, W.A., 2022. Oxidative stress, inflammation and apoptosis are the main mediators in AMB-FUBINACA induced brain injury in male Albino rats. *Azhar International Journal of Pharmaceutical and Medical Sciences* 2 (1), 82–95.
- Fakhri, S., Abbaszadeh, F., Moradi, S.Z., Cao, H., Khan, H., Xiao, J., 2022. Effects of polyphenols on oxidative stress, inflammation, and interconnected pathways during spinal cord injury. *Oxid. Med. Cell. Longev.* 2022.
- Gao, K., Shen, Z., Yuan, Y., Han, D., Song, C., Guo, Y., Mei, X., 2016. Simvastatin inhibits neural cell apoptosis and promotes locomotor recovery via activation of Wnt/ $\beta$ -catenin signaling pathway after spinal cord injury. *J. Neurochem.* 138 (1), 139–149.
- Guan, B., Chen, R., Zhong, M., Liu, N., Chen, Q., 2020. Protective effect of Oxymatrine against acute spinal cord injury in rats via modulating oxidative stress, inflammation and apoptosis. *Metab. Brain Dis.* 35, 149–157.
- Gutierrez-Zepeda, A., Santell, R., Wu, Z., Brown, M., Wu, Y., Khan, I., Link, C.D., Zhao, B., Luo, Y., 2005. Soy isoflavone glycitein protects against beta amyloid-induced toxicity and oxidative stress in transgenic *Caenorhabditis elegans*. *BMC Neurosci.* 6 (1), 1–9.
- Hu, Y.J., Gao, K.G., Zheng, C.T., Wu, Z.J., Yang, X.F., Wang, L., Ma, X.Y., Zhou, A.G., Jiang, Z.J., 2015. Effect of dietary supplementation with glycitein during late pregnancy and lactation on antioxidant indices and performance of primiparous sows. *J. Anim. Sci.* 93 (5), 2246–2254.
- Ingram, V.M., Richards, D.W., Fishman, A.P., 1962. Hemoglobin: molecular structure and function, biosynthesis, evolution and genetics. *Science* 138 (3544), 996–1000.
- Kaur, L., Singh, A., Datta, A., Ojha, H., 2023. Multispectroscopic studies of binding interaction of phosmet with bovine hemoglobin. *Spectrochim. Acta A Mol. Biomol. Spectrosc.*, 122630.
- Khan, S., Cho, W.C., Hussain, A., Azimi, S., Babadaei, M.M.N., Bloukh, S.H., Edis, Z., Saeed, M., Ten Hagen, T.L.M., Ahmadi, H., 2023. The interaction mechanism of plasma iron transport protein transferrin with nanoparticles. *Int. J. Biol. Macromol.* 124441.
- Koifman, M.O., Malyasova, A.S., Romanenko, Y.V., Yurina, E.S., Lebedeva, N.S., Gubarev, Y.A., Koifman, O.I., 2022. Spectral and theoretical study of SARS-CoV-2 ORF10 protein interaction with endogenous and exogenous macroheterocyclic compounds. *Spectrochim. Acta A Mol. Biomol. Spectrosc.* 279, 121403.
- Kong, J., Li, M., Chen, Y., Li, Y., Liu, M., Zhang, Q., Xuan, H., Liu, J., 2023. Hydrophobic interaction of four bile salts with hemoglobin induces unfolding of protein and evades protein degeneration induced by urea. *J. Mol. Liq.* 375, 121395.
- Li, M., Huan, Y., Wang, X., Tao, M., Jiang, T., Xie, H., Jisiguleng, W., Xing, W., Zhu, Z., Wang, A., 2023. Calycosin ameliorates spinal cord injury by targeting Hsp90 to inhibit oxidative stress and apoptosis of nerve cells. *J. Chem. Neuroanat.* 127, 102190.
- Li, R., Huang, L., Zhang, Z., Chen, J., Tang, H., 2022. Integrated multispectroscopic analysis and molecular docking analyses of the structure-affinity relationship and mechanism of the interaction of flavonoids with zein. *Food Chem.* 386, 132839.
- Lin, C.-C., Chen, T.-S., Lin, Y.-M., Yeh, Y.-L., Li, Y.-H., Kuo, W.-W., Tsai, F.-J., Tsai, C.-H., Yen, S.-K., Huang, C.-Y., 2013. The p38 and NF $\kappa$ B signaling protein activation involved in glycitein protective effects on isoproterenol-treated H9c2 cardiomyoblast cells. *J. Funct. Foods* 5 (1), 460–465.
- Lyndem, S., Hazarika, U., Athul, P., Bhatta, A., Prakash, V., Jha, A. N., Roy, A.S., 2023. A comprehensive in vitro exploration into the interaction mechanism of coumarin derivatives with bovine hemoglobin: Spectroscopic and computational methods. *J. Photochem. Photobiol. A Chem.* 436, 114425.
- Mandal, R., Kalke, R., Li, X.-F., 2004. Interaction of oxaliplatin, cisplatin, and carboplatin with hemoglobin and the resulting release of a heme group. *Chem. Res. Toxicol.* 17 (10), 1391–1397.
- Mariam, J., Sivakami, S., Dongre, P.M., 2017. Elucidation of structural and functional properties of albumin bound to gold nanoparticles. *J. Biomol. Struct. Dyn.* 35 (2), 368–379.

- Maurya, N., ud din Parray, M., Maurya, J.K., Kumar, A., Patel, R., 2018. Interaction of promethazine and adiphenine to human hemoglobin: A comparative spectroscopic and computational analysis. *Spectrochim. Acta A Mol. Biomol. Spectrosc.* 199, 32–42.
- Mavani, A., Ovung, A., Luikham, S., Suresh Kumar, G., Das, A., Ray, D., Aswal, V.K., Bhattacharyya, J., 2022. Biophysical and molecular modeling evidences for the binding of sulfa molecules with hemoglobin. *J. Biomol. Struct. Dyn.*, 1–12
- Nie, B.-M., Yang, L.-M., Fu, S.-L., Jiang, X.-Y., Lu, P.-H., Lu, Y., 2006. Protective effect of panaxydol and panaxynol on sodium nitroprusside-induced apoptosis in cortical neurons. *Chem. Biol. Interact.* 160 (3), 225–231.
- Nishinami, S., Arakawa, T., Shiraki, K., 2022. Classification of protein solubilizing solutes by fluorescence assay. *Int. J. Biol. Macromol.* 203, 695–702.
- Panchal, S., Sehrawat, H., Sharma, N., Chandra, R., 2023. Biochemical interaction of human hemoglobin with ionic liquids of noscapinoids: Spectroscopic and computational approach. *Int. J. Biol. Macromol.*, 124227
- Precupas, A., Leonties, A.R., Neacsu, A., Angelescu, D.G., Popa, V. T., 2022. Bovine hemoglobin thermal stability in the presence of naringenin: Calorimetric, spectroscopic and molecular modeling studies. *J. Mol. Liq.* 361, 119617.
- Qian, X., Yang, L., 2022. ROCK2 knockdown alleviates LPS-induced inflammatory injury and apoptosis of renal tubular epithelial cells via the NF- $\kappa$ B/NLRP3 signaling pathway. *Exp. Ther. Med.* 24 (3), 1–10.
- Quds, R., Hashmi, M.A., Iqbal, Z., Mahmood, R., 2022. Interaction of mancozeb with human hemoglobin: Spectroscopic, molecular docking and molecular dynamic simulation studies. *Spectrochim. Acta A Mol. Biomol. Spectrosc.* 280, 121503.
- Rao, Y., Li, J., Qiao, R., Luo, J., Liu, Y., 2023. Tetramethylpyrazine and Astragaloside IV have synergistic effects against spinal cord injury-induced neuropathic pain via the OIP5-AS1/miR-34a/Sirt1/NF- $\kappa$ B axis. *Int. Immunopharmacol.* 115, 109546.
- Sadeghzadeh, F., Entezari, A.A., Behzadian, K., Habibi, K., Amiri-Tehrani, Z., Asoodeh, A., Saberi, M.R., Chamani, J., 2020. Characterizing the binding of angiotensin converting enzyme I inhibitory peptide to human hemoglobin: Influence of electromagnetic fields. *Protein Pept. Lett.* 27 (10), 1007–1021.
- Salam, S., Arif, A., Nabi, F., Mahmood, R., 2023. Molecular docking and biophysical studies on the interaction between thiram and human hemoglobin. *J. Mol. Struct.* 1272, 134188.
- Sett, R., Paul, B.K., Guchhait, N., 2022. Deciphering the fluorescence quenching mechanism of a flavonoid drug following interaction with human hemoglobin. *J. Phys. Org. Chem.* 35 (3), e4307.
- Shahabadi, N., Zendehecheshm, S., Mahdavi, M., 2023. Exploring the In-Vitro Antibacterial Activity and Protein (Human Serum Albumin, Human Hemoglobin and Lysozyme) Interaction of Hexagonal Silver Nanoparticle Obtained from Wood Extract of Wild Cherry Shrub. *ChemistrySelect* 8 (1), e202204672.
- Shen, X.-C., Liou, X.-Y., Ye, L.-P., Liang, H., Wang, Z.-Y., 2007. Spectroscopic studies on the interaction between human hemoglobin and CdS quantum dots. *J. Colloid Interface Sci.* 311 (2), 400–406.
- Singh, D., Kaur, L., Singh, P., Datta, A., Pathak, M., Tiwari, A.K., Ojha, H., Singhal, R., 2023. Luminescence and in-silico studies of binding interactions of arylpiperazinyl-butylbenzoxazolone based synthetic compounds with bovine serum albumin. *J. Photochem. Photobiol. A Chem.* 437, 114429.
- Wang, J., Cheng, J.J., 2022. Spectroscopic and molecular docking studies of the interactions of sunset yellow and allura red with human serum albumin. *J. Food Saf.* e13030
- Wang, Y.-Q., Zhang, H.-M., Zhang, G.-C., Liu, S.-X., Zhou, Q.-H., Fei, Z.-H., Liu, Z.-T., 2007. Studies of the interaction between paraquat and bovine hemoglobin. *Int. J. Biol. Macromol.* 41 (3), 243–250.
- Yousefpour, M., Jahanbakhsh, Z., Momenzadeh, M., Mahmoudi Kelarjani, M., 2023. A Review of the Therapeutic Effect of Natural Antioxidants on Spinal Cord Injury by Focusing on Experimental Studies. *Paramedical Sciences and Military Health* 17 (2), 64–76.
- Zeinabadi, H.A., Kachooei, E., Saboury, A.A., Kostova, I., Attar, F., Vaezzadeh, M., Falahati, M., 2016. Thermodynamic and conformational changes of protein toward interaction with nanoparticles: a spectroscopic overview. *RSC Adv.* 6 (107), 105903–105919.
- Zhang, W., Cho, W.C., Bloukh, S.H., Edis, Z., Du, W., He, Y., Hu, H. Y., Ten Hagen, T.L.M., Falahati, M., 2022. An overview on the exploring the interaction of inorganic nanoparticles with microtubules for the advancement of cancer therapeutics. *Int. J. Biol. Macromol.*
- Zhang, B., Peng, J., Pan, L., Tu, K., 2023a. Exploration of molecular interaction between different plant proteins and 2-pentylfuran: Based on multiple spectroscopy and molecular docking. *J. Sci. Food Agric.*
- Zhang, B., Peng, J., Pan, L., Tu, K., 2023b. A novel insight into the binding behavior between soy protein and homologous ketones: Perspective from steric effect. *J. Mol. Liq.* 369, 120895.
- Ziberna, L., Fornasaro, S., Čvorović, J., Tramer, F., Passamonti, S., 2014. Bioavailability of flavonoids: The role of cell membrane transporters. In: *Polyphenols in human health and disease*, pp. 489–511.